

# AGN in dusty hosts: implications for galaxy evolution

M. Symeonidis<sup>1\*</sup>, J. Kartaltepe<sup>2</sup>, M. Salvato<sup>3</sup>, A. Bongiorno<sup>4</sup>, M. Brusa<sup>3</sup>, M. J. Page<sup>1</sup>, O. Ilbert<sup>5</sup>, D. Sanders<sup>6</sup>, A. van der Wel<sup>7</sup>

<sup>1</sup> Mullard Space Science Laboratory, University College London, Holmbury St. Mary, Dorking, Surrey RH5 6NT, UK

<sup>2</sup> National Optical Astronomy Observatory, 950 N. Cherry Ave, Tucson, AZ 85719, US

<sup>3</sup> Max-Planck-Institut für extraterrestrische Physik, Giessenbachstrasse 1, 85748 Garching, Germany

<sup>4</sup> INAF-Osservatorio Astronomico di Roma, via di Frascati 33, 00040 Monte Porzio Catone, Italy

<sup>5</sup> Laboratoire d'Astrophysique de Marseille, Université de Provence, CNRS, BP 8, Traverse du Siphon, 13376 Marseille Cedex 12, France

<sup>6</sup> Institute for Astronomy, 2680 Woodlawn Drive, University of Hawaii, Honolulu, HI 96822, USA

<sup>7</sup> Max-Planck-Institute for Astronomy, Königstuhl 17, D-69117, Heidelberg, Germany

Accepted Received; in original form

## ABSTRACT

We present strong empirical evidence for a physical connection between the occurrence of a starburst (SB) and a luminous AGN phase. Drawing infrared (IR), X-ray, and optically selected samples from COSMOS, we find that the locus of type-II AGN hosts in the optical colour-magnitude ( $U-V/V$ ) and colour-colour ( $U-V/V-J$ ) space significantly overlaps with that of IR-luminous ( $L_{\text{IR}} > 10^{10} L_{\odot}$ ) galaxies. Based on our observations, we propose that, when simultaneously building their black hole and stellar masses, type-II AGN hosts are located in the same part of colour-colour space as dusty star-forming galaxies. In fact, our results show that IR-luminous galaxies at  $z < 1.5$  are on average 3 times more likely to host a type-II AGN ( $L_X > 10^{42}$  erg/s) than would be expected serendipitously, if AGN and star-formation events were unrelated. In addition, the optical and infrared properties of the AGN/SB hybrid systems tentatively suggest that the AGN phase might be coeval with a particularly active phase in a galaxy's star-formation history. Interestingly, we also find a significant fraction of type-II AGN hosts offset from the dusty galaxy sequence in colour-colour space, possibly representing a transitional or post-starburst phase in galaxy evolution. Our findings are consistent with a scenario whereby AGN play a role in the termination of star-formation in massive galaxies.

## 1 INTRODUCTION

It has long been proposed that black hole growth and starburst activity follow connected evolutionary paths, inter-regulated through complex feedback processes and eventually resulting in the observed black hole – bulge relationship (e.g. Silk & Rees 1998; Magorrian et al. 1998). In the context of extragalactic studies, a popular tool for studying galaxy evolution is the rest-frame optical colour-magnitude diagram (CMD) where the position of each galaxy in colour-magnitude space is linked to its evolutionary state (e.g. Strateva et al. 2001; Baldry et al. 2004; Weiner et al. 2005). The CMD appears bimodal, where most late-types lie in the blue cloud and most early type galaxies in the red sequence, with the region between the two (the ‘green valley’; e.g. Wyder et al. 2007) being sparsely populated. The latter observation has led to the conclusion that galaxies spend only a small fraction of their lifetime in transit from the blue cloud to the red sequence, which has in turn founded speculations that energetic events associated with the central accreting black hole (active galactic nucleus; AGN), could be responsible for terminating star-formation on short timescales (e.g. Granato et al. 2004; Springel, Di Matteo &

Hernquist 2005). As a result, the search for evidence of AGN feedback in extragalactic surveys has been to a large extent pursued through examination of the properties of green galaxies and type-II AGN hosts. However, these studies have not always been in agreement with respect to whether green galaxies are a transition population or whether the colours of type-II AGN hosts are an indication of the quenching of star-formation (e.g. Westoby et al. 2007; Martin et al. 2007; Georgakakis et al. 2008; Brusa et al. 2009; Brammer et al. 2009; Schawinski et al. 2009; Cardamone et al. 2010).

Here we aim to address the topic of starburst/AGN synergy, using a sample of X-ray selected type-II AGN and a sample of  $70 \mu\text{m}$ -selected galaxies from the COSMOS  $2 \text{ deg}^2$  field. Previous work on  $70 \mu\text{m}$  populations (Symeonidis et al. 2008; 2009; 2010; Kartaltepe et al. 2010a; 2010b), has shown that the selection at  $70 \mu\text{m}$  enables the assembly of a homogeneous sample of IR-luminous ( $L_{\text{IR}} > 10^{10} L_{\odot}$ ) sources, characterised by large star-formation rates (SFRs). The motivation for this work is to investigate the link (if any) between black hole accretion and star-formation, by comparing the location of AGN hosts in the colour-magnitude, ( $U - V$  vs  $M_V$ ), and colour-colour ( $U - V$  vs  $V - J$ ) diagrams, (e.g.

Rovilos & Georgantopoulos 2007; Nandra et al. 2007; Treister et al. 2009; Hickox et al. 2009; Silverman et al. 2009; Bongiorno et al. 2012) to that of IR-luminous galaxies (Symeonidis et al. 2010; Kartaltepe et al. 2010b).

The paper is laid out as follows: in section 2 we describe the sample and in section 3 we present our results and analysis. Our conclusions are reported in section 4. Throughout, we adopt a concordance cosmology of  $H_0=70 \text{ km s}^{-1} \text{ Mpc}^{-1}$ ,  $\Omega_M=1-\Omega_\Lambda=0.3$ .

## 2 OBSERVATIONS

### 2.1 The data

Our data comes from the  $2 \text{ deg}^2$  COSMOS field (Scoville et al. 2007). The optical sample consists of 438,226 objects with  $i_{\text{auto}}^+ (\text{Subaru}) < 25$  (AB), with 30-band imaging data combined for the derivation of photometric redshifts and rest-frame magnitudes (see Capak et al. 2007; Ilbert et al. 2009). In this work we also take advantage of the  $24 \mu\text{m}$  and  $70 \mu\text{m}$  *Spitzer*/MIPS observations (Frayser et al. 2009; Le Floch et al. 2009) acquired as part of the *Spitzer* COSMOS legacy survey (Sanders et al. 2007), as well as the  $\sim 50 \text{ ks}$  *XMM-Newton* survey of the COSMOS field (Hasinger et al. 2007; Cappelluti et al. 2007; 2009). The  $70 \mu\text{m}$  catalogue used in this work together with details on the multiwavelength data cross-matching and in-depth analysis of the  $70 \mu\text{m}$  population is presented in Kartaltepe et al. (2010a, 2010b). The *XMM-Newton* X-ray catalogue is compiled and cross-matched to the optical sample in Brusa et al. (2010). There are 1550 extragalactic X-ray sources with unambiguous optical counterparts.

### 2.2 The sample

We exclude 26 per cent of the optical sample, as they have a flag which indicates that they are near a bright source, such as a star, and so their photometry might be contaminated. We also exclude from subsequent analysis the  $< 6$  per cent of sources which do not have available redshifts. Finally, we cut the 3 datasets (optical, infrared and X-ray) down to the same coverage area, leaving us with 304,627 sources in the optically-selected sample. Out of those, 1274 are detected at  $70 \mu\text{m}$  with  $f_{70} > 7.5 \text{ mJy}$  ( $> 5\sigma$ ), hereafter the IR-galaxy sample, and 1394 have  $L_X > 10^{42} \text{ erg s}^{-1}$  in either the soft or the hard-band, which we take to be our AGN sample. Note that the optical rest-frame magnitudes for the X-ray AGN come from Salvato et al. (2009) and for all other sources from Ilbert et al. (2009).

About half of the AGN have spectroscopic redshifts and the remaining have good quality photometric redshifts from Salvato et al. (2009; 2011). 27 per cent of the AGN are spectroscopically classified as broad line (BLAGN; line FWHM  $> 2000 \text{ km s}^{-1}$ ; Brusa et al. 2010). For the work presented here, we remove BLAGN, because the galaxy photometry is significantly contaminated by the active nucleus. We also exclude AGN which do not have spectroscopic redshifts, but which are classified as type-I through SED fitting to the optical photometry (see Salvato et al. 2009; Bongiorno et al. 2012). This leaves a total of 856 AGN hosts. Hereafter,

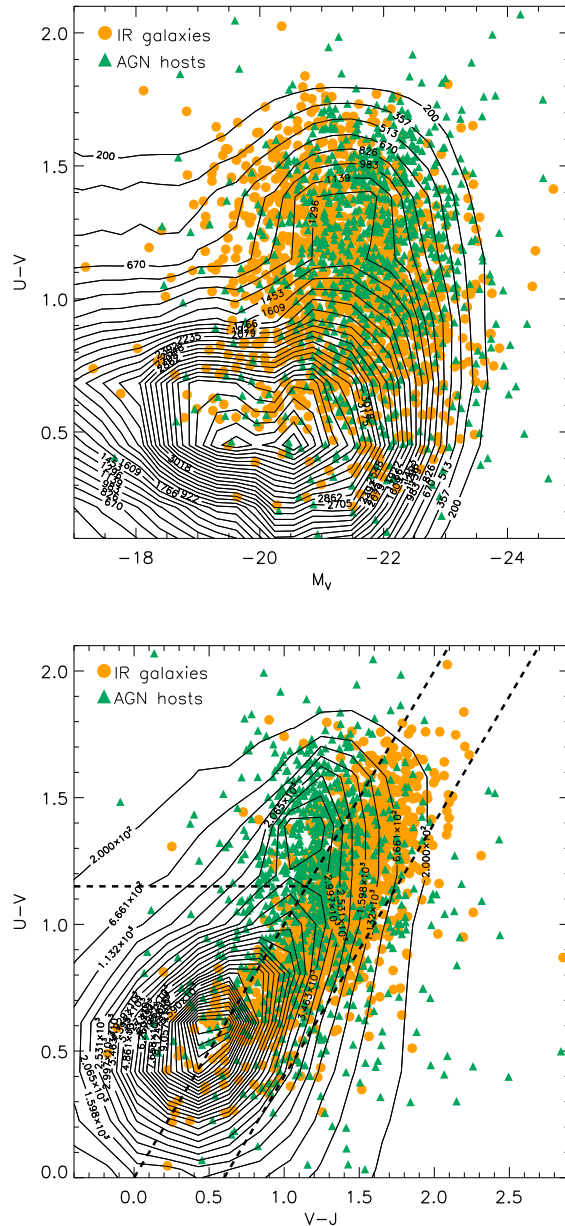


**Figure 1.** *Top panel:* The rest-frame  $U-V$  vs  $M_V$  distribution for the IR galaxy sample (orange circles) and AGN hosts (green triangles). The contours represent the number of optically-selected COSMOS sources in bins of  $0.3 \text{ mag}$  in  $M_V$  and  $0.2 \text{ mag}$  in  $U-V$ . There are 30 contours drawn in equal steps starting at 200 and ending at 4740 sources. The ‘green valley’ is around  $U-V \sim 1.1$  (see also Kartaltepe et al. 2010b). *Lower panel:* The rest-frame  $U-V$  vs  $V-J$  distribution for the IR galaxy sample (orange circles) and AGN hosts (green triangles). The contours represent the number of optically-selected COSMOS sources in bins of  $0.2 \text{ mag}$  in both axes. There are 30 contours drawn in equal steps starting at 200 and ending at 13,717 sources. The dashed lines roughly outline the region traditionally occupied by age-reddened galaxies (top left quadrant) and region of parameter space occupied by the IR-galaxy sample, the ‘dusty galaxy sequence’ (parallel lines).

when referring to AGN, it is implied that these are all type-II and hence the optical photometry is dominated by the host galaxy.

The rest-frame colour-magnitude ( $U - V$  vs  $M_V$ ) and colour-colour ( $U - V$  vs  $V - J$ ) distributions of X-ray AGN hosts and the IR galaxy sample are shown in Fig. 1, overlaid on the optically selected COSMOS population. The COSMOS sample shows a peak at blue colours ( $U - V \sim 0.5$ ; the ‘blue cloud’) and a peak at red colours ( $U - V \sim 1.3$ ; the ‘red sequence’). The transition region between the two peaks, at green ( $U - V \sim 1-1.2$ ) colours, is more sparsely populated; the so-called ‘green valley’ (see also Kartaltepe et al. 2010b). We observe a remarkable overlap between the AGN hosts and IR-galaxies as they span the same range in  $U - V$  colour and cluster at the high  $V$ -band luminosity end occupied by massive galaxies. The colours of the infrared sample are a consequence of dust reddening rather than age-related reddening, more evident in colour-colour space where age-reddened galaxies are offset from the sequence of IR galaxies (the ‘dusty galaxy sequence’), towards bluer  $V - J$  colours; see also Kartaltepe et al. (2010b); Wuyts et al. (2009); Williams et al. (2009); Whitaker et al. (2011). Particularly noteworthy is that AGN hosts lie in two camps in colour-colour space: some have colours consistent with the dusty sequence of star-forming galaxies, whereas a large fraction have bluer  $V - J$  colours, offset from the dusty galaxy sequence. These characteristics are examined in detail in section 3.

Out of the 856 type-II AGN hosts in our sample, 66 are also  $70 \mu\text{m}$  detected. In order to ensure that for these sources the  $70 \mu\text{m}$  emission is host-galaxy dominated, i.e. linked to star-formation, the  $70 \mu\text{m}$  to  $24 \mu\text{m}$  flux density ratio is used as a discriminator between AGN and star-formation dominated far-IR emission, as described in Mullaney et al. (2010). Note that this criterion can be considered reliable up to  $z \sim 1.5$ , hence we restrict all subsequent analysis to the  $0.1 < z < 1.5$  redshift range, where the lower redshift cut serves to remove local, extended sources. AGN with  $f_{70}/f_{24} > 6$  are taken to be host galaxy dominated in the infrared — 45 sources in total at  $0.1 < z < 1.5$ , hereafter referred to as the AGN/starburst (SB) hybrids. In addition, we restrict the IR galaxy sample to sources with  $f_{70}/f_{24} > 6$  in order to exclude any sources which potentially host an AGN not detected in the X-rays but dominant in the mid/far-IR. Our final sample consists of 208,512 optically-selected sources at  $0.1 < z < 1.5$ , of which 1156 are IR-emitters, 634 host AGN and 45 are AGN/SB hybrids.

Hereafter, we use the terms ‘IR galaxies’, ‘star-forming galaxies (SFGs)’ and ‘starbursts (SBs)’ interchangeably throughout this paper and ‘IR emission’ refers to infrared emission from the host galaxy linked to star-formation.

### 2.3 Sample properties

Fig. 2 shows the X-ray versus total infrared luminosity of the 45 hybrid sources, against the X-ray-Infrared correlations for star-forming galaxies taken from Symeonidis et al. (2011b) for  $L_{\text{IR}} > 10^{11} L_{\odot}$  sources (luminous and ultraluminous infrared galaxies, LIRGs and ULIRGs). To calculate X-ray luminosities, the soft and hard fluxes are  $K$ -corrected using a photon index  $\Gamma = 1.9$ , whereas the total infrared luminosities are taken from Kartaltepe et al. (2010a). We note

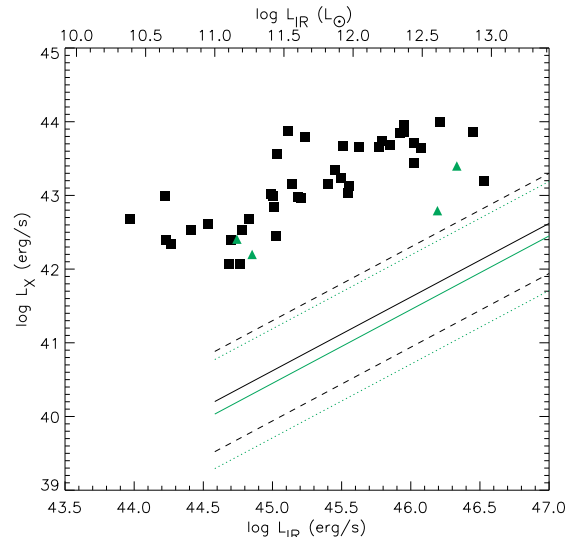


**Figure 2.** X-ray vs total infrared luminosity of the 45 AGN/SB hybrids in our final sample. When a source does not have a hard band detection (shown as a black square) then we plot its soft X-ray luminosity (shown as a green triangle). The solid lines are the X-ray/IR correlations for  $L_{\text{IR}} > 10^{11} L_{\odot}$  galaxies (LIRGs and ULIRGs) which are star-formation dominated in both the X-rays and the infrared (taken from Symeonidis et al. 2011b). The black solid and dashed lines are the *hard* X-ray-IR correlation ( $\log L_{\text{HX}} = \log L_{\text{IR}} - 4.38$ ) and  $\pm 2\sigma$  boundaries ( $\pm 0.68$  dex). The green solid and dotted lines are the *soft* X-ray-IR correlation ( $\log L_{\text{SX}} = \log L_{\text{IR}} - 4.55$ ) and  $\pm 2\sigma$  boundaries ( $\pm 0.74$  dex). Note that the AGN/SB hybrids are offset from the relations for SFGs by at least  $2\sigma$ , indicating that their X-ray emission can be assumed to be entirely AGN dominated. On the other hand their infrared emission is star-formation dominated (see main text).

that the X-ray luminosities of the hybrid sources are offset by at least  $2\sigma$  from the mean star-formation relations in the hard and soft X-ray bands. At lower infrared luminosities ( $L_{\text{IR}} < 10^{11} L_{\odot}$ ) there is some evidence that these relations might have a flatter slope (e.g. Lehmer et al. 2010), nevertheless the  $L_{\text{IR}} < 10^{11} L_{\odot}$  hybrids in our sample would still remain well above them. As a result, X-ray emission from all AGN/SB hybrids can be considered entirely AGN-dominated. In fact, in Symeonidis et al. (2010) we showed that a 200 ks X-ray survey is largely insensitive to X-ray emission from star-formation, and in the hard band even a 2Ms survey is insensitive to X-ray emission from star-formation (Symeonidis et al. 2011b), suggesting that our AGN sample is not contaminated by sources where star-formation substantially contributes or dominates the X-ray emission.

Fig. 3 shows absolute V-band magnitude as a function of redshift in the redshift range of interest ( $0.1 < z < 1.5$ ), for the optically selected sample, the AGN hosts and IR galaxies. The AGN hosts and IR galaxies are more optically luminous than the average optically-selected galaxy at each redshift, suggesting that they are also more massive as optical luminosity correlates with stellar mass (e.g. Shapley et al. 2001, Savaglio et al. 2005). Fig. 4 shows the redshift distribution of the 3 galaxy types. We note that the AGN hosts

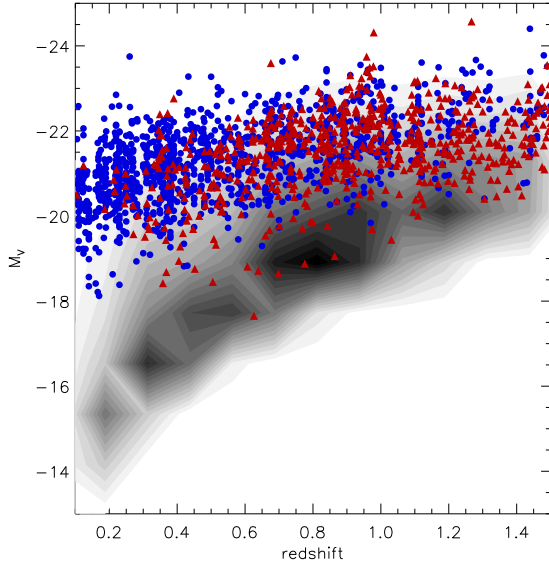


**Figure 3.** V-band absolute magnitude versus redshift for the samples used in this work — the optical population (grey filled-in contours), the AGN hosts (red triangles) and the IR galaxies (blue circles).

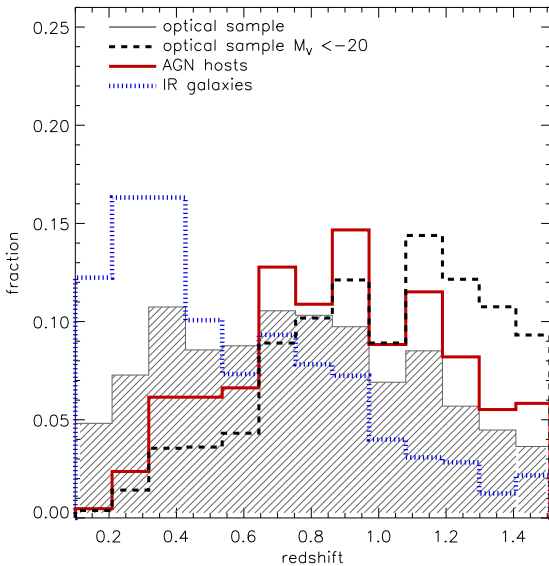


**Figure 4.** The redshift distributions of the samples used in this work. Each histogram is normalised to the total number of sources in the corresponding sample. Note that although the underlying optically-selected population has a relatively flat distribution, restricting it to the most optically bright sources ( $M_V > -20$ ) skews it towards higher redshifts.

peak at higher redshift than the IR galaxies, whereas the general population of optically-selected galaxies have a relatively flat distribution. Restricting the latter to the brightest sources with  $M_V < -20$ , which is the range in  $M_V$  probed by the AGN and IR galaxies (see Fig. 3), we find that the red-

shift distribution of the optical sample now peaks at higher redshifts, similar to the AGN hosts.

### 3 RESULTS AND ANALYSIS

#### 3.1 The distribution of AGN and IR galaxies in colour-magnitude and colour-colour space

In Figs 5 and 6 we show the colour-magnitude and colour-colour distributions for the AGN hosts and IR galaxies. They are binned and displayed as contours and further split into two redshift bins ( $0.1 < z < 0.8$  and  $0.8 < z < 1.5$ ). The overlap noted in Fig. 1 is now seen more clearly, however differences between the two populations also begin to emerge. We note that the peaks of the two distributions are well aligned in  $M_V$  but not in  $U - V$ , with AGN hosts peaking at redder colours. Moreover, many AGN hosts show bluer  $V - J$  and redder  $U - V$  colours consistent with those of red-sequence galaxies, offset to the left of the dusty galaxy sequence. These observations give weight to the notion that AGN host galaxies are not a uniform population. They also suggest that some AGN hosts have colours indicative of star-formation and dust-extinction, whereas others have colours consistent with an overall slowing down or termination of star-formation.

#### 3.2 The incidence of AGN hosted by IR galaxies

The high incidence of AGN and IR galaxies in similar parts of colour-magnitude and colour-colour space raises an important question: ‘Is it simply a coincidence?’ To address this point, we start by examining what we would expect if the answer were ‘yes’ and make the following probability argument: If AGN incidence and IR emission were independent, unrelated events in a galaxy of a given location in colour-magnitude or colour-colour space, what characteristics should the distributions of those hybrid AGN/SB sources have? To answer this question, we compute the expected number ( $N_{\text{exp}}$ ) and distribution of hybrid AGN/SB sources, under the assumption that IR-emission and AGN incidence in a given galaxy are independent events. We take binned colour-magnitude (bin size of 0.5 in  $M_V$  and 0.25 in  $U - V$ ; Fig. 5 top panel) and colour-colour distributions (bin size of 0.25 in  $V - J$  and 0.25 in  $U - V$ ; Fig. 6 top panel), allowing us to probe sources with similar optical properties (in each bin). For each bin, we count the number of optically selected sources, IR galaxies and AGN hosts and calculate the probability that an optically-selected source is both star-forming and hosts an AGN:

$$\frac{n_{i,\text{AGN}}}{n_{i,\text{opt}}} \times \frac{n_{i,\text{IR}}}{n_{i,\text{opt}}} = P_i(\text{AGN}) \times P_i(\text{IR}) = P_i(\text{AGN} \cap \text{IR}) \quad (1)$$

where  $n_{i,\text{opt}}$ ,  $n_{i,\text{AGN}}$  and  $n_{i,\text{IR}}$  are the number of optically selected galaxies, AGN and IR-selected galaxies respectively in a colour-magnitude or colour-colour bin  $i$ , and  $P_i(\text{AGN})$  is the probability that a galaxy hosts an AGN, whereas  $P_i(\text{IR})$  is the probability that a galaxy is IR-luminous and hence intensely star-forming. Subsequently we compute the expected number of galaxies in bin  $i$ , which are both IR-luminous and host an AGN:

$$N_{i,\text{exp}} = P_i(\text{AGN} \cap \text{IR}) \times n_{i,\text{opt}} \quad (2)$$

**Table 1.** Table showing the results of our experiment which compared the observed number of AGN/SB hybrids ( $N_{\text{obs}}=45\pm 6.7$ ) to the expected number of AGN/SB hybrids ( $N_{\text{exp}}$ ) computed by assuming that AGN and SF are independent events in any given galaxy (see Section 3.2). In the first column we show the redshift binning, ‘none’ indicates that the experiment is performed over the whole redshift range ( $0.1 < z < 1.5$ ) and so the samples are only binned in colour and magnitude, whereas for 2 and 4 bins, the samples are also binned in redshift. The table examines whether  $N_{\text{exp}}$  is significantly different to  $N_{\text{obs}}$ , separately for the colour-magnitude and colour-colour parameter space.  $N_{\text{exp}}$  (columns 2 and 5) is between 2 and 4 times lower than  $N_{\text{obs}}$ , indicating that type-II AGN are on average 3 times more likely to reside in dusty SFGs than would be expected serendipitously. Our calculations show that this result is significant at least at the  $3\sigma$  level and on average at the  $4\sigma$  level (columns 4 and 7). The significance is calculated by dividing the value of  $[N_{\text{obs}} - N_{\text{exp}}]$  by its uncertainty (columns 3 and 6).

redshift binning	colour-magnitude			colour-colour		
	$N_{\text{exp}}$	$N_{\text{obs}} - N_{\text{exp}}$	significance	$N_{\text{exp}}$	$N_{\text{obs}} - N_{\text{exp}}$	significance
none	$15.9\pm 1$	$29.1\pm 6.8$	$4.3\sigma$	$12\pm 0.8$	$33\pm 6.8$	$4.9\sigma$
2 bins	$18.7\pm 1.4$	$26.3\pm 6.8$	$3.8\sigma$	$12\pm 0.9$	$33\pm 6.8$	$4.9\sigma$
4 bins	$18.6\pm 1.5$	$26.4\pm 6.9$	$3.8\sigma$	$11.6\pm 1$	$33.4\pm 6.8$	$4.9\sigma$

Finally, the total number of expected hybrids  $N_{\text{exp}}$  is calculated by summing over all bins, i.e.

$$N_{\text{exp}} = \sum_i N_{i,\text{exp}} \quad (3)$$

For each bin, the error on the expected number,  $N_{i,\text{exp}}$ , is calculated by computing binomial errors on  $P_i(\text{AGN})$  and  $P_i(\text{IR})$  at the 68 per cent confidence interval ( $\sim 1\sigma$ ) and assuming no error on  $n_{i,\text{opt}}$ . The errors on  $N_{i,\text{exp}}$  from all bins are then added in quadrature to estimate the uncertainty on  $N_{\text{exp}}$ . The expected colour-magnitude and colour-colour distributions (i.e.  $N_{i,\text{exp}}$ ) are shown in Figs 7 and 8, for the whole redshift range  $0.1 < z < 1.5$  but also split into low ( $0.1 < z < 0.8$ ) and high ( $0.8 < z < 1.5$ ) redshift. In both colour-magnitude and colour-colour diagrams, the peak of the expected distribution lies at  $U - V \sim 1.1$ , indicating that the region where we would expect the highest number of AGN/SB hybrid sources to exist by chance is at green  $U - V$  colours.

Note that up to now we have not taken into account the redshift information when computing  $N_{\text{exp}}$ . As seen in Fig. 4, IR galaxies peak at lower redshifts than type-II AGN hosts and the optically selected population in the  $M_V$  range of interest. To investigate whether the differences in the redshift distributions have an impact on  $N_{\text{exp}}$ , we repeat the above process, this time also binning in redshift — i.e. bin  $i$  is now a colour-magnitude-redshift bin or a colour-colour-redshift bin. We perform the experiment with 2 redshift bins  $0.1 < z < 0.8$  and  $0.8 < z < 1.5$  and subsequently with 4 redshift bins of equal size ( $0.1 < z < 0.45$ ,  $0.45 < z < 0.8$ ,  $0.8 < z < 1.15$ ,  $1.15 < z < 1.5$ ). The computed values of  $N_{\text{exp}}$  and corresponding uncertainties are shown in table 1. We see that binning in redshift does not substantially change  $N_{\text{exp}}$  and it is difficult to say whether the small changes are due to the different redshift distributions or statistical fluctuations which come into play when binning (small number statistics).

Note that  $N_{\text{exp}}$  is higher in colour-magnitude than colour-colour space. This is because the two diagrams illustrate different galaxy properties and it is evident that there is a larger overlap between type-II AGN hosts and IR-galaxies in colour-magnitude space than in colour-colour space (see top panels of Fig. 5 and 6).

We remind the reader that observed number of hybrids ( $N_{\text{obs}}$ ) is 45 with a Poisson error of  $\sqrt{45}$  ( $=6.7$ ). To examine

**Table 2.** Table showing the significance of the K-S test performed in order to evaluate the differences in the colours and magnitudes of the observed hybrids and the expected distribution of hybrid sources (see Figs 7 and 8).

Redshift bin	Significance of K-S test			
	colour-magnitude		colour-colour	
	$M_V$	$U - V$	$V - J$	$U - V$
$0.1 < z < 1.5$	$2.5\sigma$	$1.2\sigma$	$2.4\sigma$	$1.7\sigma$
$0.1 < z < 0.8$	$2.6\sigma$	$< 1\sigma$	$2.3\sigma$	$< 1\sigma$
$0.8 < z < 1.5$	$1.3\sigma$	$< 1\sigma$	$1.1\sigma$	$< 1\sigma$

whether the difference between  $N_{\text{exp}}$  and  $N_{\text{obs}}$  is significant, we divide  $[N_{\text{obs}} - N_{\text{exp}}]$  by its corresponding uncertainty (see table 1). We find that in all cases  $N_{\text{exp}}$  is significantly lower than  $N_{\text{obs}}$  by at least  $3\sigma$  and on average by  $4\sigma$ . The ratio of  $N_{\text{obs}}$  to  $N_{\text{exp}}$  (see table 1) indicates that type-II AGN are on average 3 times more likely to reside in dusty SFGs than would be expected serendipitously. Regarding the question posed earlier, our results imply that the existence of AGN hosts and IR-luminous galaxies in the same part of colour-magnitude and colour-colour space is *not* coincidental. Instead it is likely symptomatic of a link between black hole accretion and star-formation. We speculate that this is a consequence of the large reservoirs of gas (e.g. Ivison et al. 2011) or merger events (e.g. Kartaltepe et al. 2010b; 2012) that often characterise IR-luminous galaxies, creating favourable conditions both for the AGN and star-formation.

Note that although we identify only a small number of AGN/SB hybrids, we are sampling a small part of the  $L_{\text{IR}}-z$  space, as the COSMOS  $70\mu\text{m}$  survey only picks up the most IR-luminous systems at each redshift slice, i.e. we can only detect AGN hosts with high SFRs. Lowering the SFR threshold, e.g. with a deeper  $70\mu\text{m}$  survey, might allow us to detect star-formation in a larger fraction of AGN hosts, in agreement with reports from other studies e.g. Brusa et al. (2009); Mainieri et al. (2011); Mullaney et al. (2012a), Santini et al. (2012). Nevertheless, the nature of this study, which targets the most luminous systems at each redshift slice, allows us to conclude that the incidence of luminous type-II AGN in strongly star-forming galaxies is not a serendipitous event.

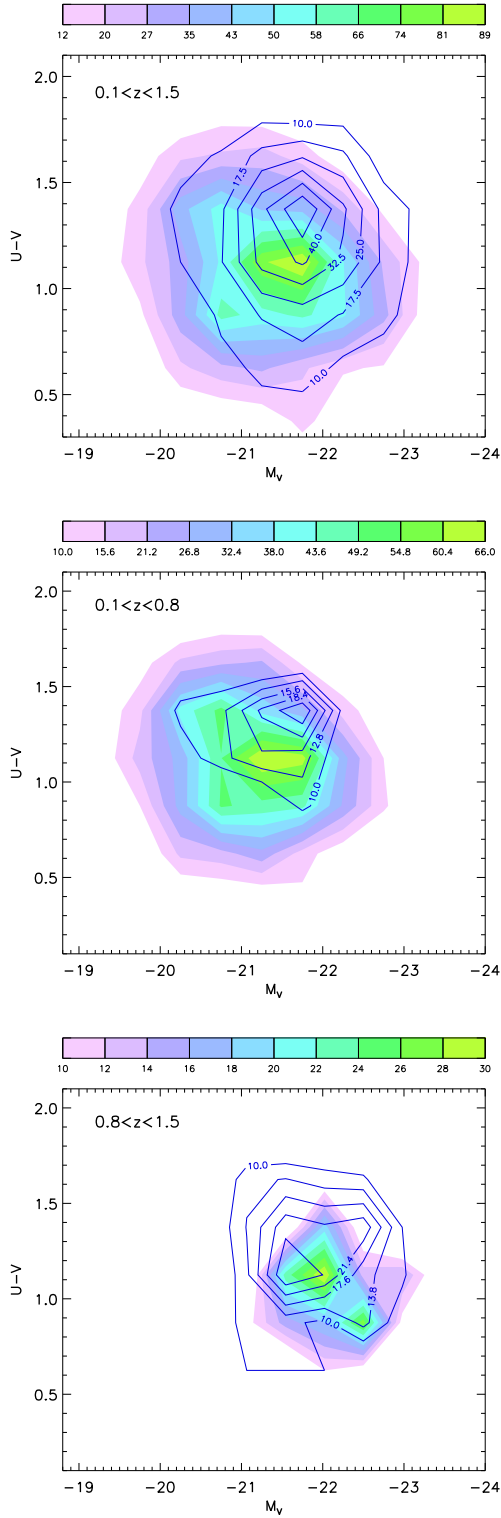


**Figure 5.** Rest-frame  $U - V$  vs  $M_V$  for the IR galaxy sample (filled contours) and AGN host galaxies (open blue contours); the 3 panels correspond to different redshift ranges. The bins are 0.5 and 0.25 in size in the x and y directions respectively and the contours represent the number of objects. 5 contour levels are drawn for the AGN and 10 contour levels for the IR-galaxies (see colour bar), starting from  $n$  number of objects, where  $n$  is either  $0.01 N$  (where  $N$  is the total number of sources) or 10, whichever is greater.

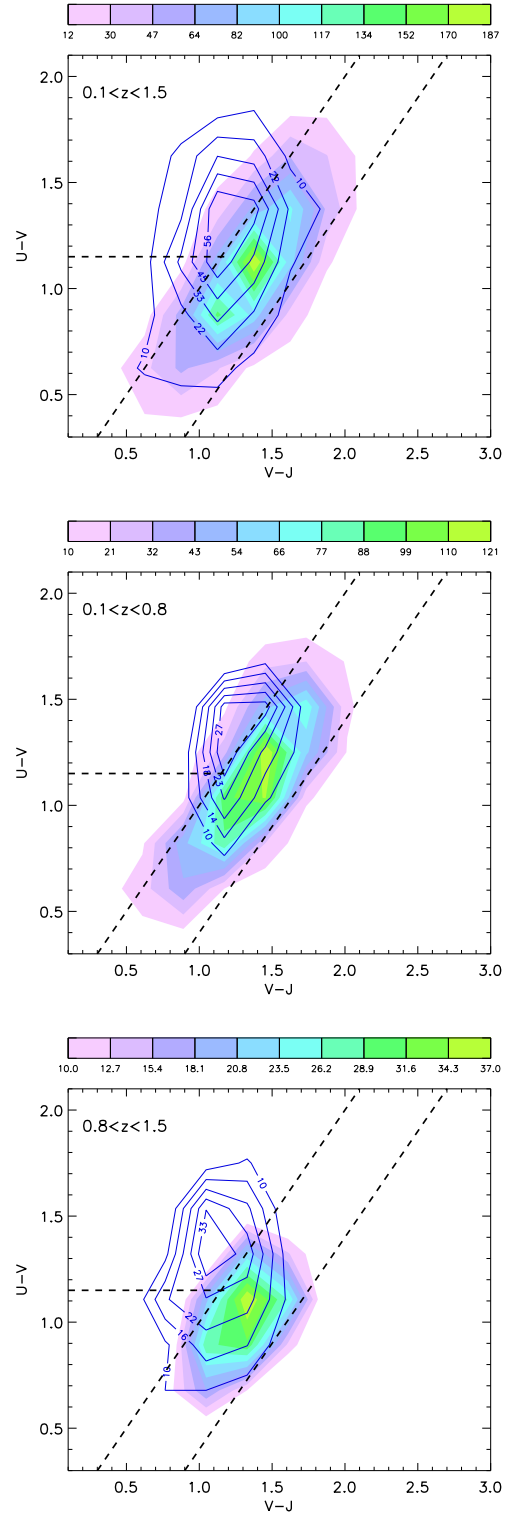


**Figure 6.** Rest-frame  $U - V$  vs  $V - J$  for the IR galaxy sample (filled contours) and AGN host galaxies (open blue contours); the 3 panels correspond to different redshift ranges. The dotted lines are the same as in Fig. 1. The bins are 0.25 in both axes and the contours represent the number of objects. 5 contour levels are drawn for the AGN and 10 contour levels for the IR-galaxies (see colour bar), starting from  $n$  number of objects, where  $n$  is either  $0.01 N$  (where  $N$  is the total number of sources) or 10, whichever is greater.

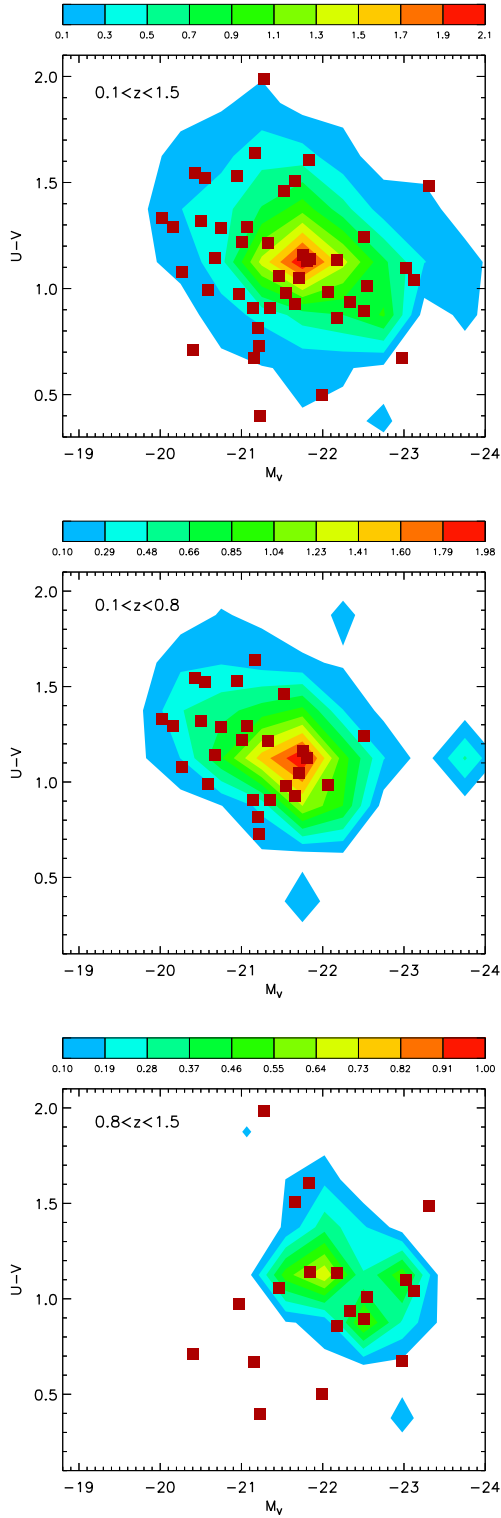


**Figure 7.** The colour-magnitude distribution expected for AGN/SB hybrids and computed under the assumption that AGN and star-formation are independent events. The total number of expected hybrids ( $N_{\text{exp}}=15.9\pm 1$  for the top panel) is calculated by summing the number of hybrids in each bin. In all panels, the bins are 0.5 and 0.25 in size in the x and y directions respectively and contours correspond to the number of sources (see colour-bar). Red squares indicate the observed distribution of AGN/SB hybrids. The 3 panels correspond to different redshift ranges.

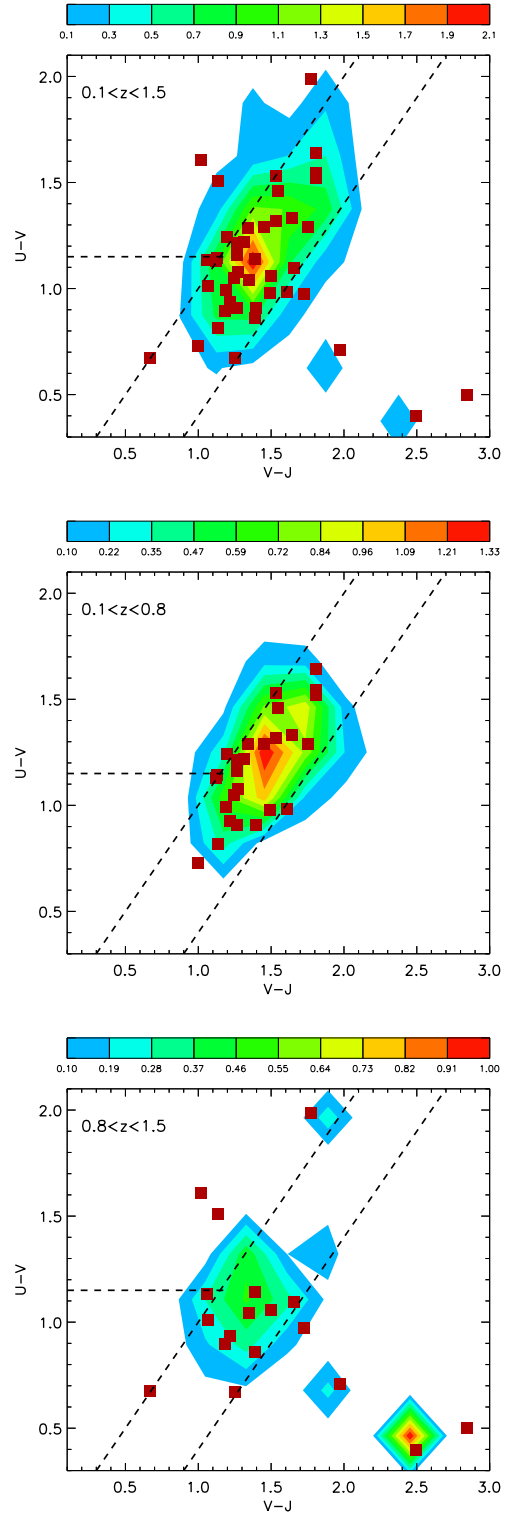


**Figure 8.** The colour-colour distribution expected for AGN/SB hybrids and computed under the assumption that AGN and star-formation are independent events. The total number of expected hybrids ( $N_{\text{exp}}=12\pm 0.8$  for the top panel) is calculated by summing the number of hybrids in each bin. In all panels, the bins are 0.25 and 0.25 in size in the x and y directions respectively and contours correspond to the number of sources (see colour-bar). Red squares indicate the observed distribution of AGN/SB hybrids. The 3 panels correspond to different redshift ranges.

### 3.3 The distribution of AGN/SB hybrids in colour-magnitude and colour-colour space

We next examine whether the connection between AGN incidence and IR-emission identified above, also manifests as a difference between the observed and expected distributions of AGN/SB hybrids, shown in Figs 7 and 8. We perform 1D K-S tests on the expected and observed distributions in  $U - V$  colour and  $V$ -band magnitude (Fig 7) and  $U - V$  colour and  $V - J$  colour (Fig 8); the results are shown in table 2. We find that the expected and observed distributions are marginally different with respect to  $M_V$  and  $V - J$ . Looking at Fig 7, we note that the  $V$ -band luminosities of the AGN/SB hybrids (particularly obvious in the low redshift bin) seem lower than expected. Similarly, Fig 8 shows that the AGN/SB hybrids are slightly offset to bluer  $V - J$  colours from the peak of the expected distribution (particularly obvious at low redshift). Although the significance of this result is marginal, it suggests that the connection between black hole accretion and star-formation, established earlier, might have an imprint on the properties of a galaxy when these processes occur simultaneously. Such hybrid sources appear to have diminished optical emission relative to IR emission and bluer  $V - J$  colours. If the reason for the former is higher obscuration, then one might expect redder  $V - J$  colours. The fact that they are bluer in combination with lower optical luminosities perhaps suggests that the AGN/SB hybrids have lower stellar masses than expected (assuming  $V$ -band luminosity to be a proxy for stellar mass). Subsequently taking the IR luminosity as a proxy for star-formation rate we infer that the AGN/SB hybrids (particularly those at low redshift) are characterised by higher specific star-formation rates (sSFRs). This suggests that the simultaneous black hole and stellar mass build up in a given galaxy potentially occurs during a particularly active phase in its star-formation history, where a large fraction of the mass is being assembled.

## 4 SUMMARY AND CONCLUSIONS

Type-II AGN hosts and IR-luminous galaxies overlap to a large extent in colour-magnitude space at green/red  $U - V$  colours ( $U - V \sim 1 - 1.5$ ) and bright  $V$ -band magnitudes ( $M_V \sim -21.5$ ), the latter of which is characteristic of massive galaxies. Large overlap between the populations is also seen in colour-colour ( $U - V$  vs  $V - J$ ) space, with many AGN lying within the region traditionally occupied by dusty SFGs. We find that within the region of overlap, type-II AGN ( $L_X > 10^{42}$  erg/s) at  $z < 1.5$  are on average 3 times more likely (with a significance of  $\sim 4\sigma$ ) to reside in dusty SFGs than would be expected serendipitously, if black hole accretion and star-formation were unrelated events. This suggests that the incidence of luminous AGN in highly star-forming galaxies is not a random event; instead it indicates a link between black hole accretion and star-formation, likely symptomatic of favourable conditions in these systems, such as large gas reservoirs and the ability to funnel gas towards the necessary regions, e.g. via mergers, bars etc. Moreover we find tentative evidence that in many sources the AGN phase is coeval with a particularly active phase in the galaxy's star-formation history, during an epoch when a large fraction of the mass is being assembled.

However the story does not end here, as besides significant overlap, we also note some clear differences in the colour-magnitude and colour-colour distributions of AGN hosts and IR galaxies. A substantial fraction of AGN hosts are offset from the parameter space occupied by dusty galaxies, displaying bluer  $V - J$  colours closer to those expected for more quiescent, post-starburst galaxies. These observations suggest that type-II AGN hosts are not a uniform population: some have colours indicative of star-formation and dust extinction, whereas others have colours indicative of the slowing down or termination of star-formation.

Although we cannot present our results as evidence of AGN feedback, we can nevertheless say that they are consistent with a scenario whereby AGN play a role in galaxy evolution. Based on our observations, we propose that massive galaxies build their black hole and stellar masses simultaneously whilst located on the dusty galaxy sequence in colour-colour space; subsequently the AGN potentially terminates star-formation, but outlives this event, and thus we observe many AGN hosts in the part of colour-colour space traditionally occupied by transitional or post-starburst systems.

## REFERENCES

- Baldry I. K., Glazebrook K., Brinkmann J., Ivezić Ž., Lupton R. H., Nichol R. C., Szalay A. S., 2004, *ApJ*, 600, 681
- Bongiorno A., et al., 2012, *MNRAS*, 427, 3103
- Brammer G. B., et al., 2009, *ApJL*, 706, L173
- Brusa M., et al., 2009, *A&A*, 507, 1277
- Brusa M., et al., 2010, *ApJ*, 716, 348
- Capak P., et al., 2007, *ApJS*, 172, 99
- Cappelluti N., et al., 2007, *ApJS*, 172, 341
- Cappelluti N., et al., 2009, *A&A*, 497, 635
- Cardamone C. N., Urry C. M., Schawinski K., Treister E., Brammer G., Gawiser E., 2010, *ApJL*, 721, L38
- Frayser D. T., et al., 2009, *AJ*, 138, 1261
- Georgakakis A., Nandra K., Laird E. S., Aird J., Trichas M., 2008, *MNRAS*, 388, 1205
- Granato G. L., De Zotti G., Silva L., Bressan A., Danese L., 2004, *ApJ*, 600, 580
- Hasinger G., et al., 2007, *ApJS*, 172, 29
- Hickox R. C., et al., 2009, *ApJ*, 696, 891
- Ilbert O., et al., 2009, *ApJ*, 690, 1236
- Iverson R. J., Papadopoulos P. P., Smail I., Greve T. R., Thomson A. P., Xilouris E. M., Chapman S. C., 2011, *MNRAS*, 412, 1913
- Kartaltepe J. S., et al., 2010a, *ApJ*, 709, 572
- Kartaltepe J. S., et al., 2010b, *ApJ*, 721, 98
- Kartaltepe J. S., et al., 2012, *ApJ*, 757, 23
- Le Floch E., et al., 2009, *ApJ*, 703, 222
- Lehmer B. D., Alexander D. M., Bauer F. E., Brandt W. N., Goulding A. D., Jenkins L. P., Ptak A., Roberts T. P., 2010, *ArXiv e-prints*
- Magorrian J., et al., 1998, *AJ*, 115, 2285
- Mainieri V., et al., 2011, *A&A*, 535, A80
- Martin D. C., et al., 2007, *ApJS*, 173, 342
- Mullaney J. R., Alexander D. M., Huynh M., Goulding A. D., Frayer D., 2010, *MNRAS*, 401, 995
- Mullaney J. R., et al., 2012, *MNRAS*, 419, 95

- Nandra K., et al., 2007, *ApJL*, 660, L11  
Rovilos E., Georgantopoulos I., 2007, *A&A*, 475, 115  
Salvato M., et al., 2009, *ApJ*, 690, 1250  
Salvato M., et al., 2011, *ApJ*, 742, 61  
Sanders D. B., others. 2007, *ApJS*, 172, 86  
Santini P., et al., 2012, *A&A*, 540, A109  
Schawinski K., Virani S., Simmons B., Urry C. M., Treister E., Kaviraj S., Kushkuley B., 2009, *ApJL*, 692, L19  
Scoville N., et al., 2007, *ApJS*, 172, 1  
Silk J., Rees M. J., 1998, *A&A*, 331, L1  
Silverman J. D., et al., 2009, *ApJ*, 696, 396  
Springel V., Di Matteo T., Hernquist L., 2005, *MNRAS*, 361, 776  
Strateva I., et al., 2001, *AJ*, 122, 1861  
Symeonidis M., et al., 2011, *MNRAS*, 417, 2239  
Symeonidis M., Page M. J., Seymour N., Dwelly T., Coppin K., McHardy I., Rieke G. H., Huynh M., 2009, *MNRAS*, 397, 1728  
Symeonidis M., Rosario D., Georgakakis A., Harker J., Laird E. S., Page M. J., Willmer C. N. A., 2010, *MNRAS*, 403, 1474  
Symeonidis M., Willner S. P., Rigopoulou D., Huang J.-S., Fazio G. G., Jarvis M. J., 2008, *MNRAS*, 385, 1015  
Treister E., et al., 2009, *ApJ*, 693, 1713  
Weiner B. J., et al., 2005, *ApJ*, 620, 595  
Whitaker K. E., et al., 2011, *ApJ*, 735, 86  
Williams R. J., Quadri R. F., Franx M., van Dokkum P., Labbé I., 2009, *ApJ*, 691, 1879  
Wuyts S., et al., 2009, *ApJ*, 700, 799  
Wyder T. K., et al., 2007, *ApJS*, 173, 293